Revista Mexicana de Astronomía y Astrofísica, **35**, 31–44 (1999)

OPTICAL TOLERANCES OF ACTIVE TELESCOPE ARCHITECTURES FOR ADAPTIVE OPTICS

Franck Marchis

European Southern Observatory, Chile

and

Salvador Cuevas

Instituto de Astronomía
Universidad Nacional Autónoma de México

Received 1998 September 24; accepted 1999 February 16

RESUMEN

Hemos estudiado cuatro diferentes arquitecturas de telescopios multi-pupilas, con área colectora equivalente a un telescopio de primario monolítico de 6.5-m, con la finalidad de encontrar la óptima para su utilización con óptica adaptativa. Las arquitecturas son: un telescopio multiespejos formado por cuatro telescopios de 3.25-m sobre la misma montura (MMMT); un telescopio cuyo espejo primario está formado por siete espejos esféricos circulares y con un secundario común (TEMOS); dos telescopios de primario segmentado tipo Keck, con 7 y 19 segmentos (TIM7 y TIM19). Mediante simulaciones de tipo Monte Carlo utilizando IDL, se hace un estudio estadístico de las tolerancias de la calidad de la óptica de los segmentos o espejos, incluyendo los defectos de "pistón" y "tip-tilt", para obtener imágenes directas limitadas por la atmósfera (80% de la luz en 0.25 segundos de arco en el visible) y para óptica adaptativa (respuesta a un impulso puntual con razón de Strehl superior a 0.8 en el visible e infrarrojo cercano). Se utiliza como referencia el telescopio Magallanes de 6.5-m por comparación y para verificar nuestro método.

ABSTRACT

We have studied four multi-pupil telescope architectures giving 6.5-m equivalent collecting diameter in order to find the optimum design for adaptive optics applications. The studied architectures are: a multi-mirror telescope with 4×3.25-m independent telescopes mounted on the same yoke (MMMT); a primary mirror composed of seven 2.7-m spherical mirrors with a common secondary (TEMOS), and two Keck type segmented telescopes with 7 and 19 segments (TIM9 and TIM19, respectively). By means of Monte Carlo simulations using IDL, we made a statistical study of the aberration optical tolerances for each telescope architecture. We included the piston and tip-tilt effects of independent individual sub-pupils. The tolerance criteria required diffraction limited telescopes in the visible and near infrared (a minimum Strehl ratio of 0.8) and, as a reference, seeing-limited imaging quality (80% light concentration in 0.25″). The same simulations were made for a 6.5-m monolithic primary mirror telescope for the purposes of comparison and verification.

Key words: **METHODS: NUMERICAL — TELESCOPES**

1. INTRODUCTION

Adaptive Optics (AO) permits nearly diffraction limited imaging of astrophysical sources in the near infrared, opening a new horizon for observational astrophysics from earth. Moreover, the point spread function (PSF) of the 3.6-m CFHT equipped with the University of Hawaii Hokupa'a 36 element AO system is cleaner and sharper than the *Hubble Space Telescope's* Point Spread Function (PSF) (Close et al. 1998). The drawback of AO is the very reduced fields, of the order of 20″.

AO systems correct a large fraction of the atmospheric turbulence seeing. Except in the case of an AO tip-tilt only corrector, the AO systems also correct the nearly static residual low order aberrations of the telescope optical train. The combined optical quality of the telescope and the AO system is nearly diffraction limited, at least for the correction wavelength. If static aberrations are relatively important, the AO system dynamic range can be affected. Fortunately, these static low order aberrations can be corrected if the telescope is active like the NTT or the WYIN telescopes.

The superb images obtained recently by the VLT1 telescope shown on the ESO home-page, proves that the active optics concept is fully operational (Wilson, Franza, & Noethe 1987). There are several classical technology telescopes that have been upgraded to include active support for the primary mirror. These telescopes achieve a better image quality. Among these telescopes is our 2.1-m telescope in San Pedro Mártir, Baja California (Cuevas et al. 1996; Salas et al. 1997).

New telescope projects include invariably active optics concepts. Furthermore, nearly all of them include AO systems. We consider that the image quality of these telescopes must not be limited only by the atmosphere, but must also be diffraction limited.

Designing an atmosphere-limited and diffraction-limited telescope with a monolithic primary is relatively straightforward. In the case of a segmented or a multi-mirror telescope, the problem is very complex. In this case low order telescope aberrations are difficult to correct with an AO system containing only one corrector mirror. The tolerances for the telescope optics are more restricted in this case.

In the case of a monolithic primary mirror, the low order aberrations that the active optics system must correct are the comatic, spherical, astigmatic, triangular, and quadratic aberrations (Wilson et al. 1987). Coma is produced mainly by the relative tip-tilt and lateral displacement between the mirror's optical axis. These adjustments are made by the secondary active mount, though coma is also produced by the primary mirror support. The others are corrected by the primary mirror support.

A segmented or a multi-mirror telescope must accomplish the same task as a monolithic one. This implies that the segments must be adjusted in such a form that the image quality under a given criterion is equivalent to that of a monolithic mirror with a superimposed mask having the segmented pupil form.

In addition to the low order aberration tolerances for the entire primary, it is necessary to know the low order aberration tolerances for each of the segments required to obtain an acceptable image quality. These aberrations are the "position" aberrations such as the piston and tip-tilt and the "shape" aberrations: astigmatic, comatic, triangular, quadratic, and spherical aberrations. These tolerances are very important for the active support design because they determine the dynamic range and precision of the actuators.

Multi-pupil primary architectures have fabrication advantages over the segmented ones. In this case, the mirrors are fabricated in axis with very well proved polishing techniques. For a segmented primary, each individual segment must be an off-axis conic, difficult to test. Furthermore, the radius of curvature for each segment must have a very reduced error, a difficult task.

At the Instituto de Astronomía of the Universidad Nacional Autónoma de México (IAUNAM) we are working on a new telescope project: the TIM telescope. This is a visible and near infrared telescope with a segmented primary of 6.5-m equivalent diameter (Salas et al. 1998). The specifications for this telescope include an AO system in the near infrared.

There are different multi-pupil primary telescope architecture concepts. Here we study how these concepts compare in image quality and low order optical tolerances. In this way, we can select the most promising architecture for the TIM project.

The tolerances are given under three different optical quality criteria. Two of these are for AO limited telescopes at the visible and near infrared. In addition, we also include seeing-limited telescope criterion. The criteria we consider are described in the next section. The telescope architectures we consider are shown in § 3. The comparison of the PSF structures in the case of perfect systems is shown in § 4. We describe our aberration simulations in § 5. In § 6, we compare the different architectures. We compare our results for the case of a monolithic telescope with the classical calculation of optical tolerances for a circular pupil optical system. We also make an estimate of the tip-tilt tolerances using a geometric approach. Our results agree very well, validating our method.

This work is a contribution to the feasibility study of TIM and, for this reason, we consider 6.5-m equivalent apertures. Future telescopes larger than 8-m will probably be segmented, so this study is also of interest for these next millennium projects.

2. IMAGE QUALITY CRITERIA

2.1. *Atmospheric Criterion*

The optical seeing at San Pedro Mártir Observatory is one of the best in the world (Echeverría et al. 1998; Avila, Vernin, & Cuevas 1998). The best values are of 0.35″ for 10% of the time. That superb atmospheric image quality should be utilized, and not degraded, by the intrinsic image quality of the telescope.

Dierickx (1992) proposed a very interesting optical quality criterion to prevent the degradation of the best seeing conditions. He shows that image quality definitions as encircled energy or FWHM makes no sense in the case of large telescopes. He introduces the Central Imaging Ratio (CIR) as the ratio of the central image spot irradiance for a telescope with aberrations in the presence of a turbulent atmosphere to the central image spot irradiance of a "perfect" telescope in the *same* turbulent atmosphere. He proposes that any telescope image quality requires CIR > 0.8. So, telescope aberrations must no disturb the image quality given by the atmosphere by more than 20%.

Making a comparison of segmented architectures using the CIR is beyond the scope of this work. Castro et al. (1998), of the GRANTECAN Optics group, have carried out such a study for a Keck-type telescope.

Instead of the Dierickx definition, we will use the optical quality of a seeing-limited telescope defined by Vernin & Muñoz-Tuñon (1992)

$$S_f{}^{5/3} = S_a{}^{5/3} + S_t{}^{5/3} \quad , \qquad (1)$$

where S_f is the FWHM of the final image, S_a the best seeing, and S_t the FWHM of the telescope's intrinsic image quality. The telescope image quality should not deteriorate S_f more than 10%, which requires $S_t \leq 0.125''$. For a Gaussian energy distribution, 80% of the encircled energy on a given diameter (d_{80}), obeys $d_{80} = 2S_t$. It follows that the intrinsic image quality of the telescope must be $d_{80} = 0.25''$.

2.2. *Adaptive Optics Criterion*

An AO system can correct atmospheric aberrations to a given order expressed in Zernike terms, depending on the system efficiency (Roddier 1998). Higher-order residuals are not corrected by the AO system. A definition similar to Dierickx's is that admitted telescope aberrations must not reduce the final Strehl ratio, given by the residual non-corrected atmospheric aberrations, by more than 20%. The Strehl ratio can be calculated using

$$S = exp\{-[(2\pi/\lambda)W]^2\} \quad ,$$

where W are the *RMS* aberrations of the system and λ the correction wavelength. This formula is valid for $S \geq 0.3$ (Racine 1996). This is the case of high order systems like ADONIS, Pueo, or Hokupa'a (Rousset et al. 1994; Rigaut et al. 1998; Graves & Northcott 1998). If W_t and S_t are the aberrations and the Strehl ratio of the telescope alone and W_a and S_a are the residual non-corrected atmospheric aberrations and the Strehl ratio obtained by the AO system, the combined telescope and AO system Strehl ratio is given by $S = S_a S_t$. It is clear that if $S_t \geq 0.8$, the total Strehl ratio will not be affected more than 20%. This obeys the classical definition given by Maréchal (Maréchal & Françon 1970).

We choose as the correction wavelengths 0.55 μm and 1.25 μm, corresponding to AO systems working in the visible and the NIR. The last value is the wavelength specified for the AO system for the TIM telescope (Cuevas et al. 1998).

3. SEGMENTED TELESCOPE ARCHITECTURES

The use of many small mirrors combined to make a single telescope of large collecting area was proposed by Steinheil 141 years ago (Steinheil 1857). Some months before, Foucault (1857) described the precursor of all the monolithic modern astronomical telescopes: the silvered glass telescope.

Recent telescope projects can be divided into three groups: monolithic primary telescopes, segmented primary telescopes, and multi-mirror telescopes with single or multiple secondaries. Among the segmented telescopes the best known are the Keck I and Keck II telescopes and the Scandinavian 25-m project (Nelson, Mast, & Faber 1985; Arderberg et al. 1996).

The Large Binocular telescope is a multi-mirror telescope and has a precedent in the NOAO National New Technology Telescope (NNTT) project (Hill 1990; Barr et al. 1983; Wolf et al. 1982). This telescope was a natural extrapolation of the MMT telescope, which has been an optical bench for very useful experiments in cophasing control (Beckers & Williams 1978; Lloyd-Hart et al. 1993).

Another telescope architecture is the TEMOS (TElescope MOSaic) from the Marseilles Observatory (Baranne & Lemaitre 1980, 1987). It is a telescope with a primary composed by 4 or 6 circular spherical mirrors with a common active curvature secondary.

It is very difficult to compare the different architectures. For that reason we limit this study to the optical specifications for the primary segments or for the primary mirrors. We propose some " basic" representative architectures of each type:

1. A monolithic primary telescope such as the Magallan 6.5-m project. We considered it to have a 0.678 m secondary. This telescope is also a reference for imaging quality and for verifying our simulations.

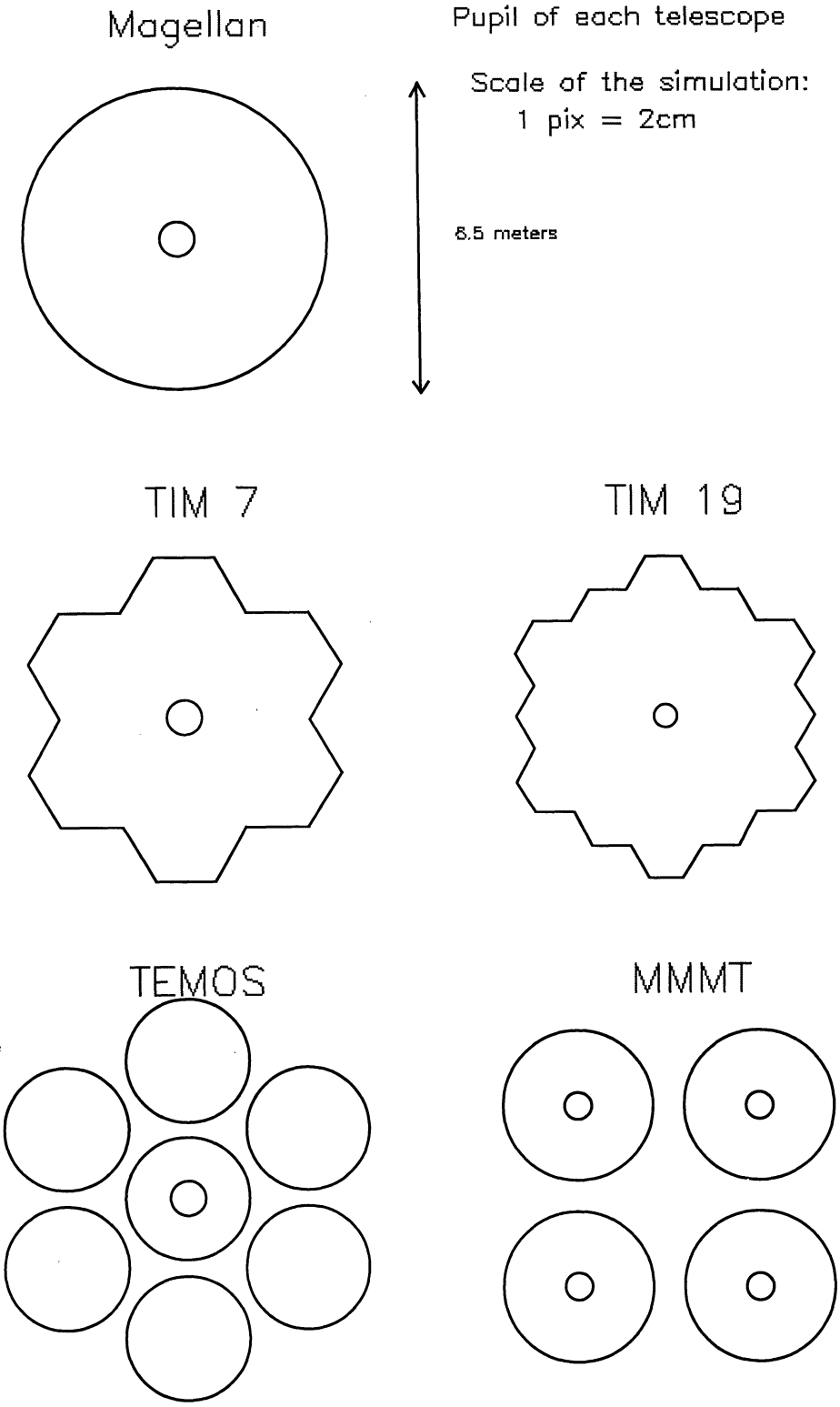

Fig. 1. The geometry of telescope pupils for different architectures. Magellan is a monolithic 6.5-m telescope. TIM7 and TIM19 are Keck type telescopes with 7 and 19 segments, respectively. TIM7 has 2.7 m diameter inscribed hexagons. TIM19 has 1.6 m diameter inscribed hexagons. These telescopes have a 0.678 m diameter secondary. TEMOS has 7 circular (spherical) mirrors with a common 0.687 m secondary. MMMT is a multi-mirror 4 × 3.25-m telescope. Each mirror has its own 0.5 m secondary.

2. We study two segmented 6.5-m equivalent telescope architectures, scaling down the Keck telescope. One of them has seven 2.7 m diameter hexagonal segments. The other one has nineteen 1.6 m hexagonal segments. We named these architectures TIM7 and TIM19, respectively.

3. A multi-mirror telescope composed of four 3.25 m circular mirrors mounted on the same yoke, each one with its own 0.5 m secondary. We named this telescope the Mexican Multi-Mirror Telescope (MMMT). This is, in fact, a model of the NNTT project.

4. A TEMOS type telescope with seven 2.7 m mirrors and a common 0.678 m secondary. We chose this configuration in order to compare it with the TIM7 architecture.

We suppose that any IR instrument attached to these telescopes has a cold pupil masking the background radiation that comes from hot parts other than the mirrors. If the telescopes have an alt-azimuth mount, the instrument must rotate to compensate for the field rotation. The cold pupil must be de-rotated because the telescope pupil does not rotate with the field. We suppose also a correct baffling of the telescopes at visible wavelengths.

4. PERFECT TELESCOPE COMPARISONS

We can compare the pupil of the five proposed architectures. Figure 1 shows the pupil configuration of the telescopes. The holes correspond to the secondaries.

The pupil function for a monolithic primary mirror telescope is defined by

$$P(\vec{u}) = \begin{cases} 1, & \text{if } |\vec{u}| \leq D/2\lambda \\ 0, & \text{otherwise} \end{cases} , \qquad (2)$$

where $\vec{u}$ is a position vector, λ the wavelength, and D the telescope diameter.

In the case of the MMMT and the TEMOS type telescopes the pupil function is defined by

$$P(\vec{u}) = A(\vec{u}) * \sum_{j=1}^{N} \delta(\vec{u} - \vec{u}_j) \quad , \qquad (3)$$

where the operator $*$ denotes a convolution, $\delta(\vec{u})$ is the Dirac delta function, $\vec{u}_j$ is the position vector of each mirror center, and $A(\vec{u})$ is defined in a similar form as for a round pupil

$$A(\vec{u}) = \begin{cases} 1, & \text{if } |\vec{u}| \leq d/2\lambda \\ 0, & \text{otherwise} \end{cases} , \qquad (4)$$

where d is the sub-pupil diameter and N is the number of mirrors in the pupil ($N = 4$ for the MMMT and $N = 7$ for the TEMOS).

In the case of the TIM7 and TIM19 telescopes the $A(\vec{u})$ function in equation (3) can be substituted by a convenient hexagon function $H(\vec{u})$. The number N in these cases is $N = 7$ and $N = 19$, respectively, and

$$P(\vec{u}) = H(\vec{u}) * \sum_{j=1}^{N} \delta(\vec{u} - \vec{u}_j) \quad . \qquad (5)$$

From these pupil functions, the telescope Point Spread Function (PSF) is calculated using a squared Fourier transform: $PSF_{perf}(\vec{u}) = |TF(P(\vec{u}))|^2$. In this case, the PSF is dependent only upon the geometry of the pupil. Although it is possible to calculate the PSF of each of the pupils analytically, we choose to calculate them numerically. The calculation was made over an 800 × 800 array. Each pixel represents 2 cm in the real telescope pupil. In order to compare the PSF's, it was necessary to make an area normalization.

In Figure 2 we plot the resulting PSFs using a logarithmic grayscale. We can see that the PSFs for the TIM7 and TIM19 telescopes present a secondary lobe whose hexagonal symmetry is caused by the irregular pupil edge. The secondary lobes are more important in the case of the TIM19 pupil. For the TEMOS and MMMT designs, these secondary lobes are negligible.

It is difficult to compare the architectures in a quantitative form. For this reason, we calculated a circular mean for each PSF. The calculation was made in polar coordinates: $\vec{u} = \vec{e_r} + \vec{e_\theta}$. The mean PSF is expressed as $PSF_{moy}(r) = \langle PSF(r,\theta) \rangle_\theta$. Figure 3 shows a linear scale representation of all the mean PSFs. The Magellan and TIM telescopes have very similar PSFs. The MMMT and the TEMOS have a narrower PSF but they have important secondary maxima.

The TEMOS can be compared with the TIM7, which has the same number of constituent mirrors for the primary. The TEMOS produces a better energy distribution PSF. The MMMT has a slightly better resolution but only in two diagonal directions, where the baseline is longer. The secondary maxima and the hexagonal lobes can be removed by deconvolution during image processing.

In Table 1, the relative Strehl ratio between all the segmented architectures are compared taking the Magellan telescope as a reference. The difference in this ratio is negligible in all the cases.

In the absence of aberrations there are no practical differences between the different telescope architectures.

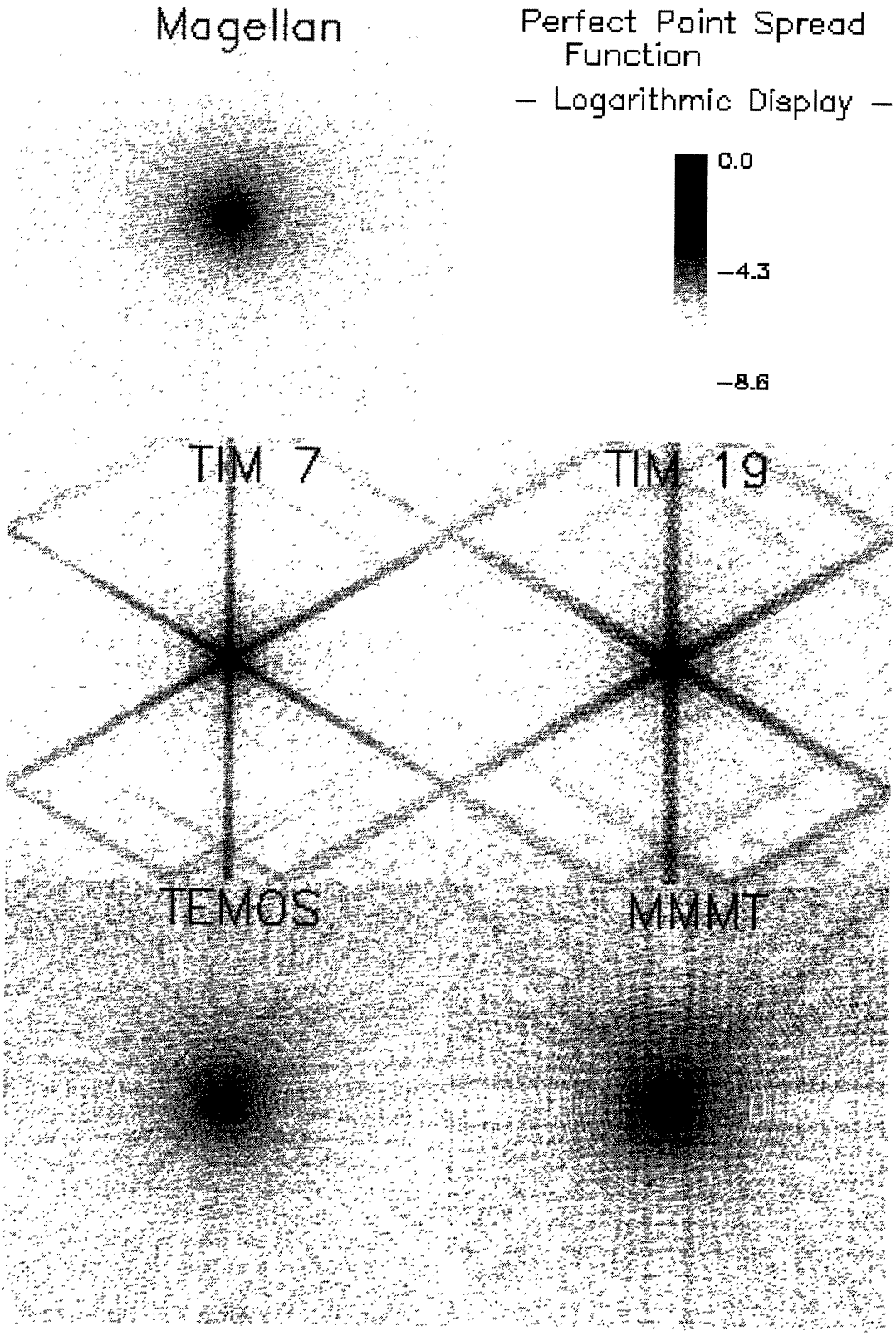

Fig. 2. Logarithmic grayscale PSF representation. TIM7 and TIM19 have lobes with an hexagonal symmetry. The difference between Magellan and the MMMT and TEMOS is negligible.

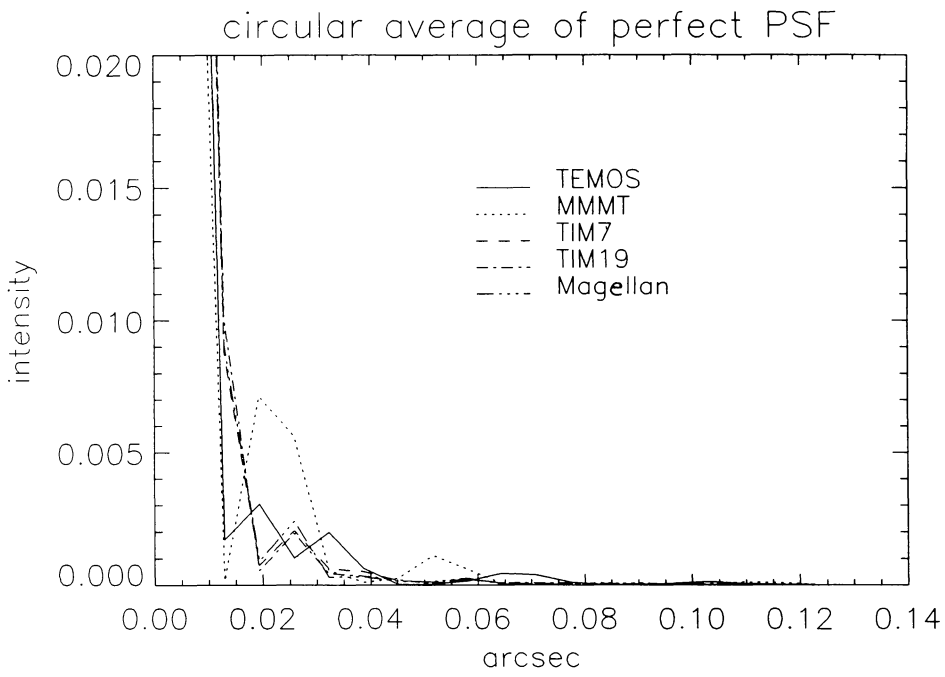

Fig. 3. Circular mean of the PSFs.

5. ABERRATIONS: CALCULATION METHOD

Although the calculation of the PSFs for the different architectures in the absence of aberrations is easy, a calculation of the PSFs in the presence of aberrations is not a simple task. Here, we calculate the PSF for each architecture as a combination of the aberrations presented by each segment or mirror.

For a monolithic mirror telescope the complex pupil function $P(\vec{u})$ is now described by

$$P(\vec{u}) = \begin{cases} e^{\frac{2i\pi}{\lambda}W(\vec{u})}, & \text{if } |\vec{u}| \leq D/2\lambda \\ 0, & \text{otherwise} \end{cases} , \quad (6)$$

where $W(\vec{u})$ is a function describing the phase of the aberrations in linear units.

TABLE 1

RELATIVE STREHL RATIO[a]

Telescope	Relative Strehl Ratio
MMMT	0.8258
TEMOS	1.0140
TIM7	1.0117
TIM19	1.0456

[a] Taking Magellan as the reference.

$W(\vec{u})$ can be described by means of an expansion of Zernike polynomials if $\vec{u}$ is given in polar coordinates ρ, θ (Born & Wolf 1964).

$$W(\rho,\theta) = \sum_{i=1}^{n} a_i Z_i(\rho,\theta) \quad . \quad (7)$$

For a multi-mirror telescope, the complex pupil function can be described by a superposition of complex sub-pupils

$$P(\vec{u}) = A_j(\vec{u}) * \sum_{j=1}^{N} \delta(\vec{u} - \vec{u}_j) \quad , \quad (8)$$

where $A_j(\vec{u})$ is the complex sub-pupil function defined similarly to the round pupil of the Magellan telescope with aberrations. The aberrations over each sub-pupil have different values

$$A_j(\vec{u}) = \begin{cases} e^{\frac{2i\pi}{\lambda}W(\vec{u})}, & \text{if } |\vec{u}| \leq d/2\lambda \\ 0, & \text{otherwise} \end{cases} . \quad (9)$$

In both of the TIM cases, the sub-pupil complex function is described by a Zernike expansion over a round pupil. After that, the complex function is cut in hexagonal form. The complex pupil function is similar to equation (8) using a convenient hexagonal sub-pupil $H_j(\vec{u})$.

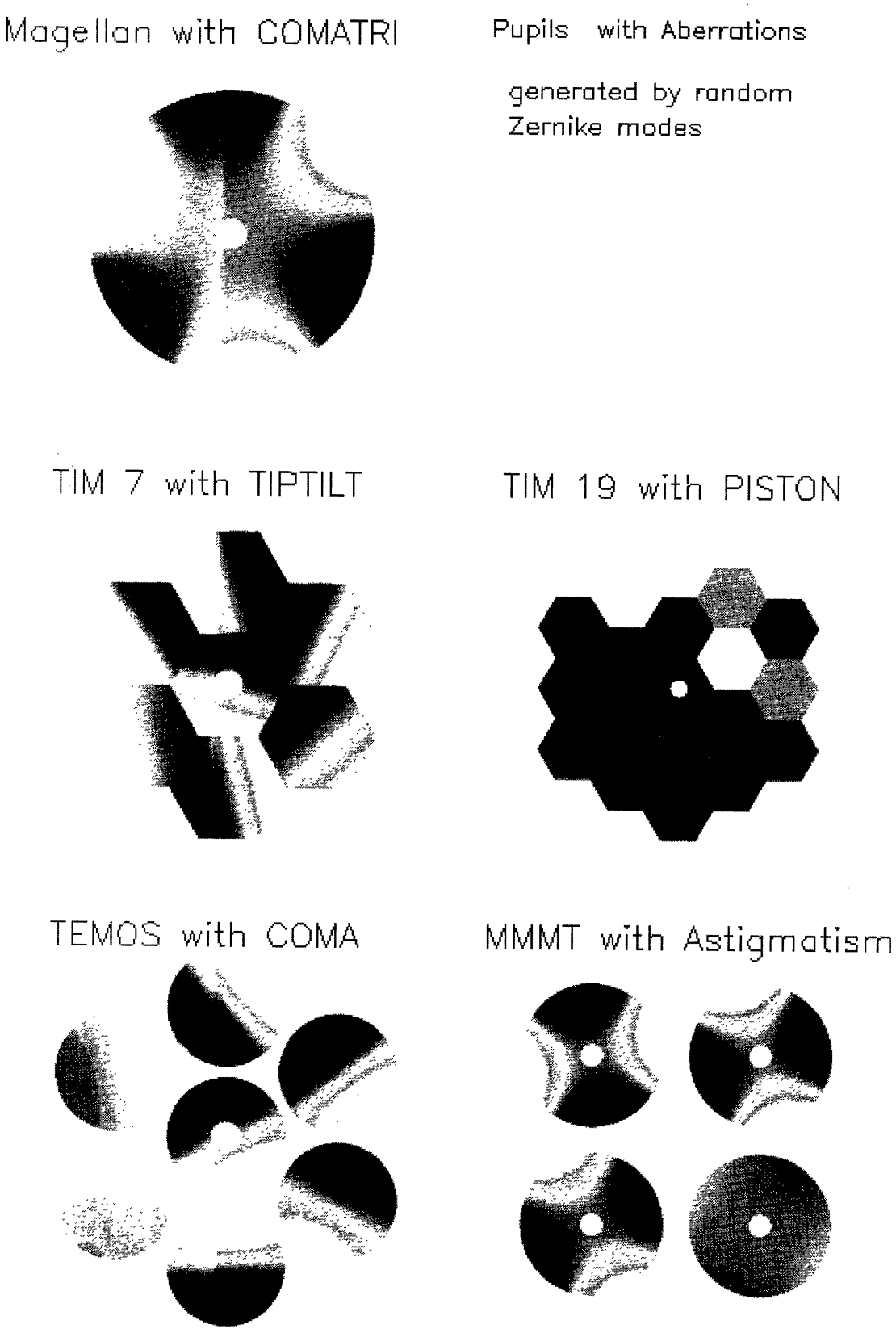

Fig. 4. A grayscale representation of the Zernike aberrations.

The PSF of each telescope architecture with aberrations can be calculated in analytical form for the Magellan, the MMMT, and TEMOS architectures, using the Fourier transform properties of Zernike polynomials. The analytical calculation for the TIM telescope types with aberrations is very difficult. For that reason, we made numerical calculations by means of fast Fourier transforms using the IDL© language.

The origin of each aberration for the segments or mirrors is different. We calculated only "pure" aberrations in each case, in order to understand the PSF behavior. Figure 4 illustrates an example of one aberration class on each telescope architecture.

- The Piston position aberration corresponds to the Zernike term Z_1. It introduces only a phase difference in each mirror or segment.
- A relative tip-tilt in each sub-pupil corresponds to Z_2, Z_3. Like the piston aberration, is a "position" aberration.
- The astigmatism, given by Z_5 and Z_6 is the lowest energy deformation aberration. This is the principal aberration that an active support must correct.
- Triangular coma is present in all telescope mir-

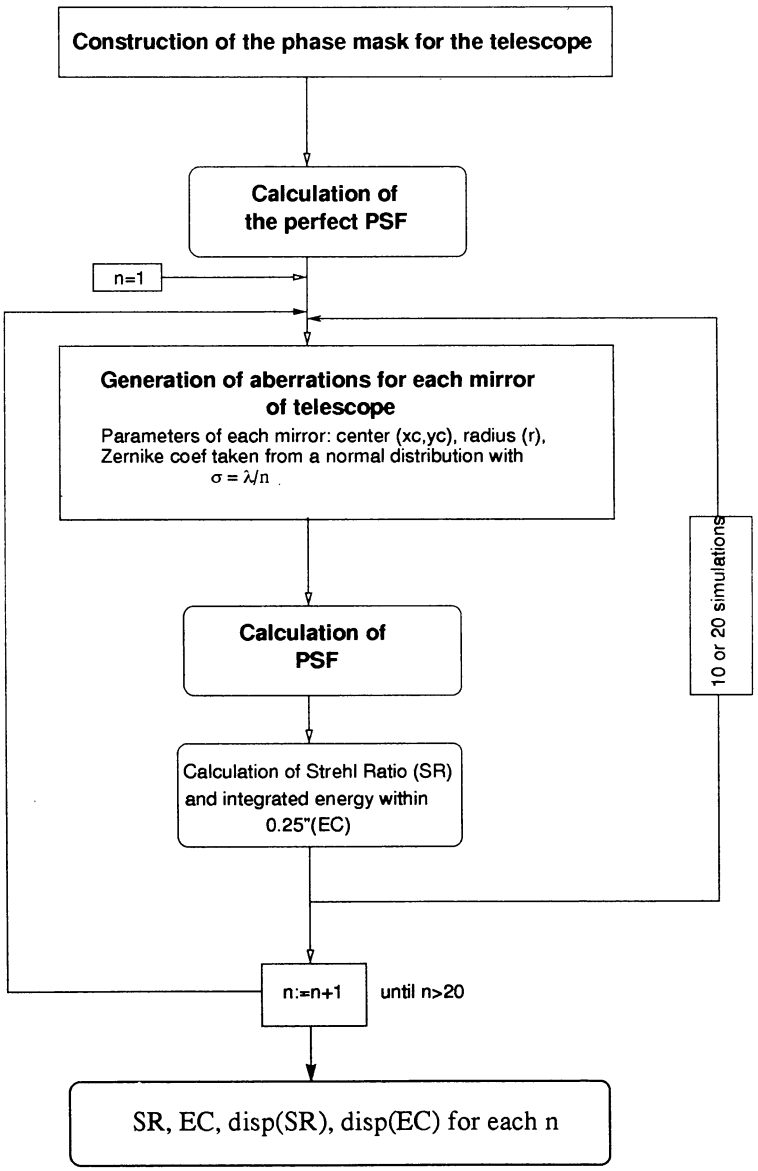

Fig. 5. Monte Carlo simulations procedure. SR =Strehl Ratio; EC = Integrated energy concentrated within $0.25''$. These values were calculated from 10 or 20 simulations. The dispersions ($\pm$ 3σ) for SR ($disp[SR]$) and EC ($disp[EC]$) were calculated from the same data.

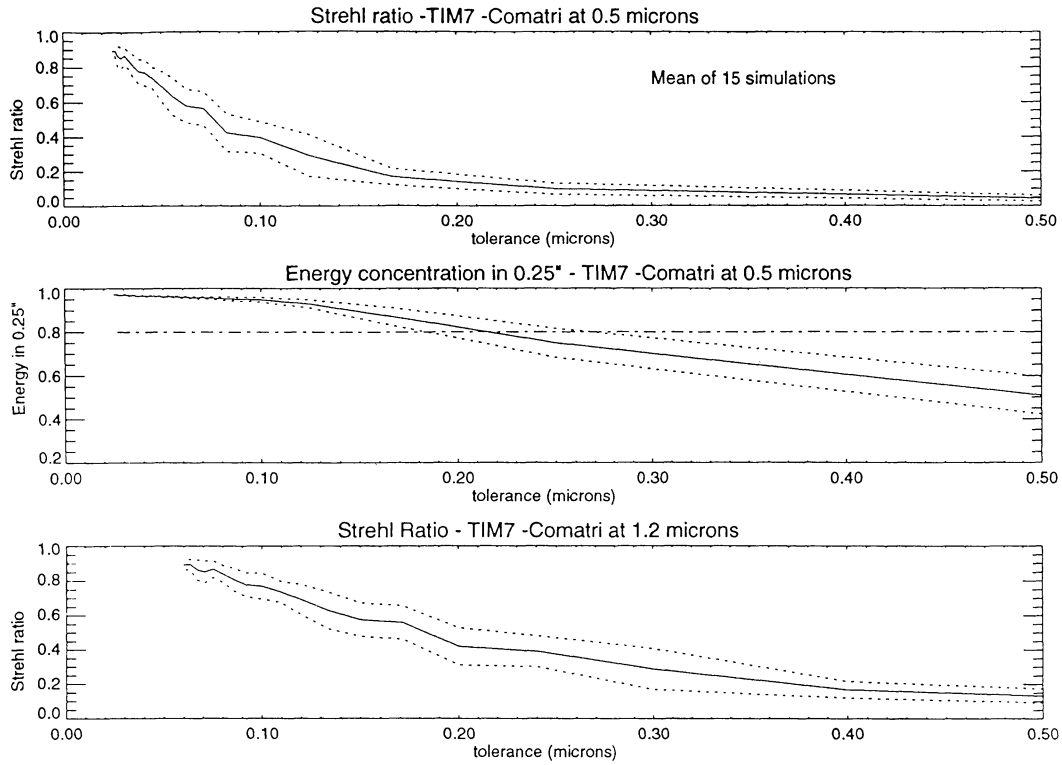

Fig. 6. Simulation results of Comatri for the TIM7 type telescope.

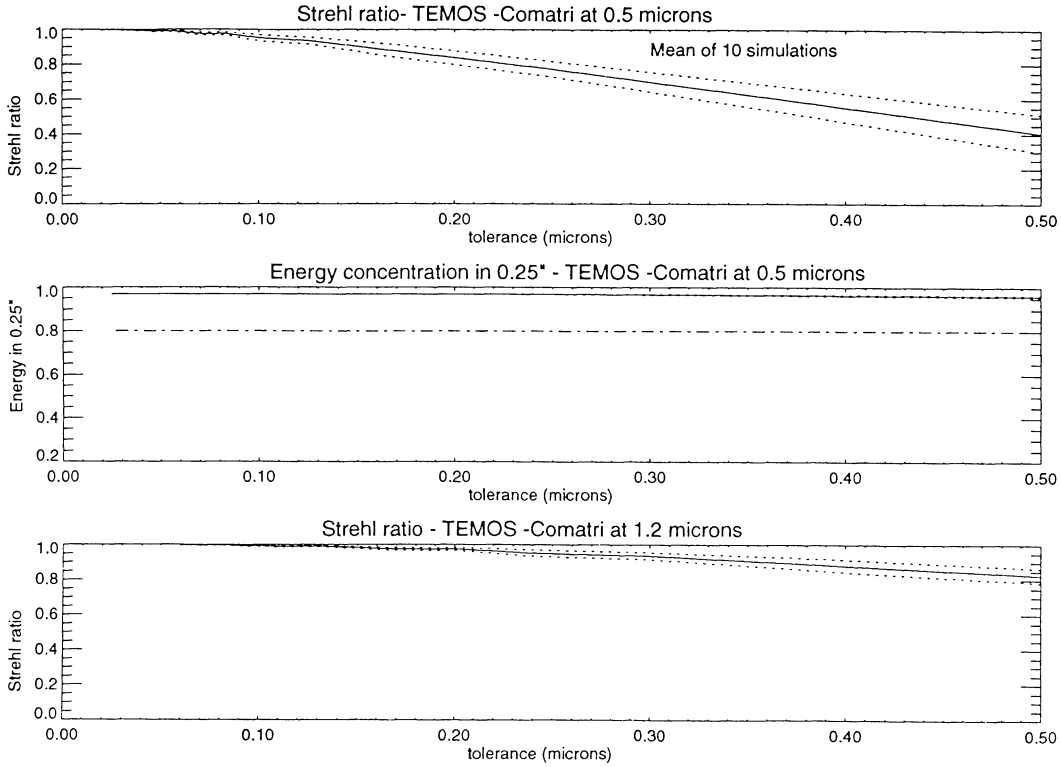

Fig. 7. Simulation results of Comatri for the TEMOS telescope.

rors. The origin of this deformation aberration is the three position definition points in the mirror support system. It will be present on each segment of the architectures studied. This aberration is described by the Z_9 and Z_{10} Zernike terms.

• The coma aberration is very dependent upon the telescope type. It is given by a mirror deformation and by the primary and secondary mirror misalignment. In the case of a monolithic mirror the coma is compensated by actively aligning the secondary unit. In the other architectures, the coma for each segment or mirror must be compensated primarly by the active segment supports.

6. MONTE CARLO SIMULATIONS

Our principal interest is to determine the aberration tolerances of each telescope architecture under the three image quality criteria. In order to have representative results, we used a Monte Carlo approach. We generated random Zernike coefficients, as it is indicated in § 5, distributed with a Gaussian distribution around zero for each one of the mirrors or segments. The width $\sigma = \lambda/n$ ($\lambda = 0.50$ μm) for $n = 1$ to $n = 20$ of the Gaussian distribution represents the associated error for each aberration type. Ten or twenty simulations were made for each n value. For each simulation, the Strehl ratio of the PSF's were calculated using the perfect mirror PSF as a reference. The mean Strehl ratio (SR) of the 10 or 20 simulations were plotted as a function of σ. The same procedure was made when calculating the integrated energy concentrated within $0.25''$ (EC). This procedure is illustrate in Figure 5.

The simulations were made for all of the studied telescope architectures and for the five pure aberrations. We also calculated a Piston and tip-tilt combination.

The Zernike terms used here are those defined by (Noll 1975). Two examples of our simulations are shown in Figures 6 and 7, where the SR and EC is plotted as a function of the triangular coma for the TIM7 and the TEMOS telescopes. These telescopes have 7 segment or mirrors on a similar geometrical distribution. The TEMOS architecture has more relaxed tolerances than the TIM7 architecture for this aberration. The dispersion ($\pm$ 3σ) of the SR values or EC is plotted in dashed lines.

7. RESULTS

7.1. *Seeing Limited Tolerances*

Table 2 contains the results of the simulations for the different architectures and for all the aberrations for telescopes limited by "seeing", that is $d_{80} = 0.25''$. The aberration values are given in microns. Since the Zernike polynomials are normalized according to Noll, these values are wavefront RMS values. In surface aberrations, these values must be divided by 2 and divided by the corresponding Noll normalization factor if the peak to valley value is needed. The dispersion of the obtained mean values is indicated. Tip-tilt and Piston have no meaning for the monolithic primary (Magellan).

The results are nearly identical for similar telescope types. The MMMT and the TEMOS have similar tolerance values, as do the segmented TIM7 and TIM19. An important result is that the tip-tilt tolerances are more restrictive than the Piston tolerances in all the cases. The tolerances for the multi-mirror telescopes are more relaxed than those for the segmented telescopes.

We made a PSF analysis for all the architectures. The energy is spread in the secondary lobes near the PSF center for low aberration values. For the same aberration value, this energy is spread more quickly in the case of segmented mirrors than in the case of multi-mirror architectures. This can be explained as follows. The telescope PSF is the superposition (for the seeing-limited criterion) or the interference (for the AO criterion), on the common focus, of the individual PSF's provided by each segment or individual mirror. Present aberrations on each element spread the energy over the individual PSF. This energy is more spread on hexagonal mirrors than on circu-

TABLE 2

RMS ABERRATION TOLERANCES IN μm FOR SEEING-LIMITED TELESCOPES[a]

Telescope	Piston	TT	TT+Piston	Astig.	Coma	Tri
Magellan	...	...	...	0.4 ± 0.1	0.2 ± 0.1	≥ 1
MMMT	≥ 1	≥ 1	≥ 1	≥ 1	0.55 ± 0.08	≥ 1
TEMOS	≥ 1	≥ 1	≥ 1	≥ 1	0.38 ± 0.06	≥ 1
TIM7	≥ 1	0.33 ± 0.08	0.30 ± 0.1	0.28 ± 0.04	0.16 ± 0.03	0.22 ± 0.04
TIM19	≥ 1	0.21 ± 0.04	0.21 ± 0.02	0.16 ± 0.01	0.122 ± 0.006	0.13 ± 0.01

[a] $d_{80} = 0.25''$. The ($\pm 3\sigma$) dispersion of the tolerances is indicated.

lar mirrors. The final superposition (or interference) has lower energy in the central part for segmented than for multi-mirror telescopes. A manifestation of this phenomenon can be inferred from Figs. 6 and 7, where equal number of elements (7 segment or mirrors) architecture tolerances are shown.

The tolerances obtained for the multi-mirror telescopes are of the same order as the aberrations present in the passive telescopes (Roddier et al. 1994). For passive telescopes, the astigmatic, comatic, and triangular aberrations have typical *RMS* values of 213nm, 186nm and 84nm, respectively. Thus it is possible to build passive support, multi-mirror telescopes that are seeing-limited.

The case of the segmented telescopes is different. The aberration values correspond to an active support mirror like the 2.1-m SPM telescope (Cuevas et al. 1996; Salas et al. 1997). Typical aberration *RMS* values for this UNAM instrument for astigmatism, coma, and the triangular aberration are 6nm, 100nm, and 98nm, respectively. The conclusion here is that segmented telescopes require active support of the segments if the complete optics is to be seeing-limited.

The astigmatism sensitivity is 1.7 times larger for the TIM19 than for the TIM7. For a seeing-limited segmented telescope, it is better to design it with segments as big as possible.

It is necessary to point out that it is not correct to compare the deformation aberrations with the corresponding values for the Magellan telescope. For the Magellan telescope, these aberrations are for the complete pupil, and, for the other architectures, they correspond to each segment or mirror.

The piston and tip tilt tolerances are of the order of 1λ in wavefront for segmented telescopes. This tolerance is at least a factor of 2 larger for the multi-mirror telescopes. Controlling the position of 1.5 m mirror or segments to within a 1 μm error can be a very difficult task.

7.2. *NIR AO Tolerances*

The tolerances for the AO in the NIR are the central purpose of this work. Table 3 contains the tolerances for this case.

The tip-tilt tolerances in all cases are very similar and slightly more restrictive than the Piston tolerances. As in the seeing-limited case, the segmented

TABLE 3

RMS ABERRATION TOLERANCES IN μm FOR A DIFFRACTION-LIMITED TELESCOPE AT 1.25 μm[a]

Telescope	Piston	TT	TT+Piston	Astig.	Coma	Tri
Magellan	...	...	...	0.07 ± 0.03	0.07 ± 0.01	0.18 ± 0.04
MMMT	0.13 ± 0.06	0.12 ± 0.03	0.08 ± 0.01	0.24 ± 0.05	0.06 ± 0.01	≥ 1
TEMOS	0.09 ± 0.02	0.13 ± 0.02	0.08 ± 0.02	0.25 ± 0.06	0.06 ± 0.02	≥ 1
TIM7	0.10 ± 0.02	0.07 ± 0.01	0.054 ± 0.007	0.078 ± 0.001	0.07 ± 0.01	0.09 ± 0.01
TIM19	0.09 ± 0.01	0.072 ± 0.005	0.058 ± 0.003	0.08 ± 0.01	0.073 ± 0.003	0.091 ± 0.007

[a] Strehl ratio > 0.8. The ($\pm 3\sigma$) dispersion of the tolerances is indicated.

TABLE 4

RMS ABERRATION TOLERANCES IN μm FOR A DIFFRACTION-LIMITED TELESCOPE AT 0.5 μm[a]

Telescope	Piston	TT	TT+Piston	Astig.	Coma	Tri
Magellan	...	...	...	0.02 ± 0.01	0.03 ± 0.01	0.08 ± 0.02
MMMT	0.06 ± 0.02	0.05 ± 0.01	0.033 ± 0.006	0.12 ± 0.02	0.026 ± 0.005	0.22 ± 0.06
TEMOS	0.040 ± 0.006	0.054 ± 0.008	0.035 ± 0.007	0.12 ± 0.02	0.028 ± 0.005	0.23 ± 0.03
TIM7	0.04 ± 0.01	0.028 ± 0.004	0.022 ± 0.003	0.032 ± 0.005	0.030 ± 0.005	0.038 ± 0.005
TIM19	0.04 ± 0.007	0.030 ± 0.003	0.024 ± 0.002	0.033 ± 0.004	0.030 ± 0.004	0.038 ± 0.007

[a] Strehl ratio > 0.8. The ($\pm 3\sigma$) dispersion of the tolerances is indicated.

telescopes have more restrictive tolerances than the multi-mirror telescopes. The values for the tip-tilt and Piston tolerances are at least one order of magnitude lower than for seeing-limited telescopes. Controlling the positions of the segments or mirrors inside this error range will be a severe challenge for the future segmented telescopes in AO applications.

The values for the deformation aberrations in almost all cases correspond to typical values of telescopes with active supported primaries. Exceptions are the triangular tolerances for the multi-mirror telescopes. The image quality does not seem to be very sensitive to this aberration in these telescopes. The active support technology for segmented telescopes currently exists, for AO applications.

7.3. *Visible AO Tolerances*

Table 4 summarizes our results for the AO criterion for $\lambda = 0.5$ μm. The results are, as expected, more restrictive than the NIR AO tolerances. If diffraction limited imaging at visible wavelengths is to be accomplished, the tight tolerances will persuade the engineers not to use a segmented telescope.

7.4. *Verification of our Results*

7.4.1. Deformation Aberrations

The values obtained for the Magellan architecture were used to verify our simulations. The classical criterion establish that a system is diffraction limited if the Strehl ratio value is larger than 0.8 (Maréchal & Françon 1970). This Strehl ratio can be obtained if the *RMS* aberrations $W \leq \lambda/14$. This corresponds to 85nm for $\lambda = 1.2$ μm and 36nm for $\lambda = 0.5$ μm. This is in agreement with the obtained tolerance values for the AO in the NIR and the visible (Tables 3 and 4).

7.4.2. Tip-Tilt Aberration

It is possible to make a geometrical estimate for the tip-tilt tolerances for the multi-mirror telescopes.

In the seeing-limited image quality case, the individual mirror images must be superposed within a circle of 0.25″ diameter. The wavefronts coming lower than half this value. The tip-tilt Zernike terms measure the distance, in linear dimensions, from the wavefront and a reference plane at the pupil edge. This distance is given by $d \times 312 \times 10^{-9}$, where d is the sub-pupil diameter, with the conversion factor from radians to arcsecs introduced. For 3.25 m or 2.7 m mirrors, these distances are 1 μm and 0.525 μm, respectively. There is a factor of 2 given by the Noll normalization so, these values must be doubled. The Zernike terms obtained in this form are in agreement with the values in Table 2 for the MMMT and TEMOS architectures.

The same estimations can be made for the diffraction limited case. The individual images coming from each individual mirror must superpose in the focal plane with a precision given by the PSF radius *FWHM* of the largest base B of the telescope (8.7 m for the MMMT and 8.6 m for the TEMOS). This is given by $\lambda/2B$. The Zernike coefficients for the tip-tilt for the MMMT and the TEMOS at 1.25 μm are 115nm and 97nm, respectively, in agreement with our results in Table 3. From these estimations we are confident that our simulations are correct.

8. CONCLUSIONS

The principal goal in this work was to determine the aberration tolerances for the individual segments from the segments must have a relative inclination of four different multi-pupil telescope architectures for AO applications.

The telescopes studied were a 7 and a 19 segment Keck type telescope (TIM7 and TIM19), a 4 mirror multi-mirror telescope (MMMT), and a 7 mirror TEMOS type telescope. A monolithic primary mirror telescope was also simulated in order to verify our results.

- The criterion for AO applications was that the telescopes must be diffraction limited for the correction wavelength. We also calculated these tolerances for seeing-limited image quality.
- The tolerances for the TIM7 and TIM19 telescopes are independent of the segment number for AO applications. It is better to use big segments in the case of seeing-limited telescopes.
- Multi-mirror telescopes have more relaxed tolerances than the TIM-type in both the AO criteria and seeing-limited image quality.
- The tolerances obtained for deformation aberrations (astigmatism, coma, triangular aberration) are of the order of the residual aberrations in monolithic active support primary telescopes. That means that all telescope types must have active segment support in order to achieve the image quality imposed by the two criteria.
- For the piston and tip-tilt aberrations the resulting values are a real challenge for present telescope technology.

We thank the Instituto de Astronomía UNAM, for the financial support to F. Marchis in México before he left for Chile. We wish to thank V. Voitsekhovich for stimulating discussions about the "philosophical" problem of the quality of telescope optics. We are indebted to Claude and François Roddier for pointing out that the TEMOS is a multi-pupil telescope. Finally, we are grateful to M. Richer and D. Ojeda for his help in the translation from our Spanish-French English text to a legible English one. *Ihuan omochiuh in tlanextli.*

REFERENCES

Arderberg, A., Andersen, T., Jessen, N. C., & Owner-Petersen, M., 1996, Optical Telescopes of Today and Tomorrow, ed. A. Arderberg, Proc. SPIE 2871 (Bellingham, WA: SPIE Press), 585

Avila, R., Vernin, J., & Cuevas, S. 1998, PASP, 110, 1106

Baranne, A., & Lemaitre, G. 1980, C.R. Acad. Sci. Paris, 291 série B-39

_____. 1987, C.R. Acad. Sci. Paris, 305 série II, 445

Barr, L. D., Lynds, C. R., Angel, J .R. P, Wolf, N. J., Mast, T., & Nelson, J. E. 1983, Advanced Technology Optical Telescopes II, ed. L. D. Barr, Proc. SPIE 444 (Bellingham, WA: SPIE Press), 37

Beckers, J. M., & Williams, J. T. 1978, Advanced Technology Optical Telescopes I, ed. L. D. Barr & G. Burbidge, Proc. SPIE 332 (Bellingham, WA: SPIE Press), 2

Born, M., & Wolf, E. 1964, in Principles of Optics (New York: Pergamon Press), 464

Castro, F. J., Bello, C. D., Jochum, L., & Devaney, N. 1998, Advanced Technology Optical/IR Telescopes VI, ed. L. M. Stepp, Proc. SPIE 3352 (Bellingham, WA: SPIE Press), 386

Close, L. M., Roddier, F., Roddier, C. Graves, J. E., Northcott, M., & Potter, D. 1998, Adaptive Optical Systems Technologies, ed. D. Bonaccini & R. K. Tyson, Proc. SPIE 3353 (Bellingham, WA: SPIE Press), 406

Cuevas, S., Martínez, L. A., Iriarte, A. Harris, O. & Roddier, C. 1996, Technical Report RT-01-96, Instituto de Astronomía, UNAM

Cuevas, S., et al. 1998, Adaptive Optical System Technologies, ed. D. Bonaccini & R. K. Tyson, Proc. SPIE 3353 (Bellingham, WA: SPIE Press), 531

Dierickx, P. 1992, J. of Modern Optics, 39, 569

Echeverría, J., et al. 1998, RevMexAA, 34, 47

Hill, J. M. 1990, Advanced Technology Optical Telescopes IV, ed. L. D. Barr, Proc. SPIE 1236 (Bellingham, WA: SPIE Press), 86

Foucault, L. 1857, C.R. Acad. Sci. Paris, 44, 339

Graves, J. E., & Northcott, M. J. 1998, Adaptive Optical System Technologies, ed. D. Bonaccini & R. K. Tyson, Proc. SPIE 3353 (Bellingham, WA: SPIE Press), 34

LLoyd-Hart, M., Dekany, R., McLeod, B., Wittman, D., Colucci, D., McCarthy, D., & Angel, R. 1993, ApJ, 402, L81

Maréchal, A., & Françon, M. 1970, in Diffraction, Structure des Images (Paris: Masson & Cie.), 108

Nelson, J., Mast, T., & Faber, F. 1985, Advanced Technology Optical Telescopes III, ed. L. Barr, Proc. SPIE 628 (Bellingham, WA: SPIE Press), 207

Noll, R. J. 1975, J. Opt. Soc. Am., 66, 207

Racine, R. 1996, PASP, 108, 372

Rigaut, F., et al. 1998, PASP, 110, 152

Roddier, F. 1998, PASP, 110, 837

Roddier, C., Graves, J. E., Northcott, M. J., & Roddier, F. 1994, Advanced Technology Optical Telescopes V, ed. L. M. Stepp, Proc. SPIE 2199 (Bellingham, WA: SPIE Press), 1172

Rousset, G., et al. 1994, Adaptive Optics in Astronomy, ed. M. A. Ealey & F. Merkle, Proc. SPIE 2201 (Bellingham, WA: SPIE Press), 1088

Salas, L., et al. 1997, App. Opt., 36, 3708

Salas, L., et al. 1998, Advanced Technology Optical/IR Telescopes VI, ed. L. M. Stepp, Proc. SPIE 3352 (Bellingham, WA: SPIE Press), 44

Steinheil, C. 1857, C.R. Acad. Sciences, 45, 968

Vernin, J., & Muñoz-Tuñon, C. 1992, A&A, 257, 811

Wilson, R. N., Franza, F., & Noethe, L. 1987, J. of Modern Optics, 34, 485

Wolf, N. J., Angel, J. R., Antebi, J., Carleton, N., & Barr, L. D. 1982, Advanced Technology Optical Telescopes, ed. L. D. Barr & G. Burbidge, Proc. SPIE 332 (Bellingham, WA: SPIE Press), 79

Salvador Cuevas: Instituto de Astronomía, UNAM, Apartado Postal 70-264, 04510 México, D.F., México (chavoc@astroscu.unam.mx).

Franck Marchis: European Southern Observatory, Alonso de Córdova 3107 Vitacura P.O. 19001 Santiago 19, Chile (marchis@eso.org).